Talanta 186 (2018) 133–139

Contents lists available at ScienceDirect

Talanta

journal homepage: www.elsevier.com/locate/talanta

Quantitative study of the mineralogical composition of mineral dust aerosols by X-ray diffraction

Sophie Nowak[a,*], Sandra Lafon[b], Sandrine Caquineau[c], Emilie Journet[b], Benoit Laurent[b]

[a] Plateforme Rayons X, UFR de Chimie, Université Paris Diderot, Paris, France
[b] Laboratoire Interuniversitaire des Systèmes Atmosphériques (LISA), UMR 7583, Université Paris Diderot, Université Paris-Est Créteil, IPSL, Créteil, France
[c] Laboratoire d'océanographie et du climat: expérimentations et approches numériques (LOCEAN), Sorbonne Universités, UPMC, CNRS, IRD, MNHN, Bondy, France

ARTICLE INFO

Keywords:
Mineralogical composition
Mineral dust particles
Powder X-Ray Diffraction
Rietveld analysis

ABSTRACT

Mineral dust aerosols, produced by wind erosion in arid regions and semi-arid surfaces, are important components of the atmosphere that affect the Earth radiative budget, atmospheric chemistry and biogeochemical cycles. Dust aerosol particles are composed of a complex mixture of various minerals, mainly clays, calcite, quartz, feldspars and iron oxides. The nature and the relative abundance of the minerals are key parameters to evaluate mineral dust environmental impacts. Strong limitations remain to quantify the mineralogical composition of dust particles, mainly due to the low mass of in-situ collected dust particle samples. In this study, an analytical method and X-Ray Diffraction (XRD) measurements are presented to quantify the mineralogical composition of low mass aerosol particle samples. The method is applied on reference minerals (illite, kaolinite and palygorskite) commonly present in desert dust aerosols, as well as on lab-generated dust aerosols from desert soils. XRD measurements of theses samples in rotation in a glass capillary are combined with the Rietveld refinement method. The results obtained are repeatable and confronted to theoretical values given in the literature for the reference minerals. This method allows us to quantify the mineralogical composition of low mass dust mineral samples with an unprecedented accuracy.

1. Introduction

Mineral dust particles production by wind erosion on arid and semi-arid surfaces amounts for about 40% of the global annual emissions of aerosols in the troposphere [24], with a major contribution from North Africa where the Sahara and the Sahel are located [40]. These particles, with diameters commonly below tens of microns, are composed of a variety of minerals, e.g. clays, calcite, quartz, feldspars, iron oxides, etc., of which the relative abundances vary by source region [20,42,5]. The mineralogical composition of dust particles controls their optical properties [17,38,47], as well as their ability to serve as cloud condensation nuclei and ice nuclei [50], and their reactivity in the atmosphere [30]. The iron solubility of dust particles, a key issue to estimate its bioavailability, is also highly dependent on its mineralogical form [11,25,43]. It is essential to investigate the dust mineralogical composition and its regional variability in detail, in order to improve our understanding of the impact of dust on the environmental [19,33,42,44].

Aerosol samples collected on filters typically do not exceed few milligrams. This limits the accurate characterization of their particulate mineral composition by direct methods (based on crystallographic properties) due to incompatibility of these low mass samples with most analytical techniques commonly being used. Alternative indirect methods based on reconstruction of the mineralogy from elemental composition or radiative properties are often applied. Also, mineralogical compositions were obtained from bulk elemental analysis or individual particles analysis [15,16,18,26,27,33].

A direct measurement of the mineralogical composition of mineral samples can be performed by X-Ray Diffraction (XRD), but only the relative masses of the mineral phases reported to the crystallized fraction of the sample can be determined. The amorphous or badly crystalized compounds cannot be detected and it is therefore not possible to assess the total mass of the sample. Even if the XRD analysis is never quantitative in an absolute way, it is considered as "quantitative" or "semi-quantitative" according to the method used. Regarding "semi-quantitative" information, XRD users consider that the calibration methods based on fluctuant parameters, such as the so called Reference Intensity Ratio (RIR) correcting the signal from the X-ray absorption, make that a unique measured signal is not obtained for a given sample preparation nor a given instrument. The standard deviation on the

* Corresponding author.
E-mail address: sophie.nowak@univ-paris-diderot.fr (S. Nowak).

https://doi.org/10.1016/j.talanta.2018.03.059
Received 22 November 2017; Received in revised form 20 March 2018; Accepted 21 March 2018
Available online 22 March 2018
0039-9140/

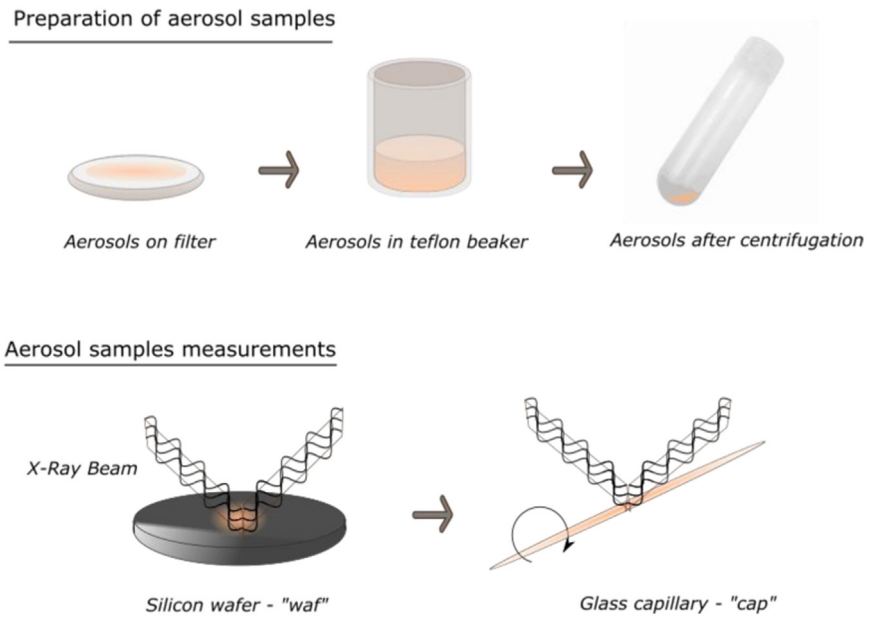

Fig. 1. Schematic representation of the preparation steps of the aerosol samples and the XRD analysis on a silicon wafer and in a glass capillary.

calibration is therefore unknown and cannot provide more than a "semi-quantitative" result. The obtained composition could only be compared from one sample to another from a given analyze set. However, "quantitative" methods integrate the influence of the instrument, the absorption of the phases, etc. These quantitative measurements can be obtained by using internal standards or by the Rietveld refinement method. The addition of an internal standard is not appropriate for low mass samples, such as dust aerosol samples on filters, due to large inaccuracies. The Rietveld method is based on the treatment of the whole pattern [41] and is commonly used by the XRD community. It is considered as the best way to determine a lot of information from a powder diffractogram [48] but requires that measurements are made on specimens with random orientation in order to determine the relative intensities of different peaks [14]. Nonetheless, it is difficult to obtain randomly oriented mineral particles from low-mass samples of dust particles. The detection of clay minerals, one of the main phases of dust aerosols, remains problematic. Indeed, these clay minerals show only very weak reflections in randomly oriented particle samples, more so they are present in low concentrations in the samples. Both their identification and quantification remain difficult due to their anisotropic particle shape and their crystal structure [39].

Caquineau et al. [4] developed an original preparation method that allows analyzing by XRD atmospheric dust particles collected on polycarbonate filters. It involves transferring the particles from the polycarbonate filter to a porous ceramic slide (Si), a substrate suitable for XRD analysis. This leads to lower background and enhanced peak intensities for the main mineral species, but induces slight preferred orientations of the clay minerals. A semi-quantitative treatment based on the method of Chung [9] with calculated RIR factors were then applied but only to some of the detected minerals (illite, kaolinite and quartz). Kandler et al. [27] also developed a qualitative and semi-quantitative approach by XRD to characterize the mineralogical composition of desert dust collected on filters. The identification of clay minerals deposited onto a silicon wafer is improved due to preferred orientation, whereas relative mineral contents are calculated from spectra obtained on randomly oriented powder samples using the method of Chung [9]. More recently, Klaver et al. [28] developed a method by which the particles collected on filters are extracted and deposit on a silicon wafer. This was followed by a semi-quantitative analysis (based on calibration curves established from reference minerals) of only the non-clay phases.

To date only semi-quantitative XRD methods had been applied to dust aerosol samples. We present here a new procedure that allows the quantification of the mineralogical composition of dust samples, and avoids the limitations due to the low aerosol mass and to the clay mineral content of the sample. This procedure is adapted to the analysis of samples with less than few milligrams of mineral particles on polycarbonate filters. The measurements are done in two steps, enabling (i) the identification of the mineral phases in the samples, and (ii) their quantification based on a Rietveld refinement procedure applied to the aerosol particle samples.

2. Material and methods

Atmospheric desert aerosol samples collected during field campaigns are often a complex mixture of various soil minerals and organic particles. Quantities of desert particulate matter collected on filters as well as their mineral compositions could vary substantially from one sample to another. In order to develop and test our analytical procedure, we choose to work on reference and laboratory generated (under controlled conditions) samples constituting dust aerosol particles. This approach allows us to verify if the minerals are being correctly analyzed. Also this allows us to work with samples of few milligrams having particle size typical of natural aerosols, and to repeat the measurements under controlled conditions. Three reference clay minerals documented in the literature, and two desert soils were chosen to generate filter samples, similar in mass to ambient aerosols.

A preliminary XRD measurement was performed on the sample deposited from the filter on a flat silicon (Si) monocrystalline wafer. The particles extraction from the sampling media and deposition on the flat silicon wafer was performed following the method by Caquineau et al. [4]. Thereafter the sample was transferred into a glass capillary tube and a second XRD measurement performed. The capillary analysis can then be performed on very small quantities of sample by rotating the capillary mounted sample. This avoids a preferred orientation of the minerals and provides intensity ratios close to the theoretical values for all minerals. From these measurements, the quantitative mineralogical composition of the dust particles can be determined by Rietveld refinement [14]. The steps on the preparation of the samples and of their subsequent analyses are summarized in Fig. 1.

2.1. Aerosol generation in laboratory

The clay mineral references selected for this study are illite, kaolinite and palygorskite. The illite and kaolinite are the most widespread and the most abundant clay mineral species in dust aerosol particles. They are detected in samples and their cumulative contents can reach 70% of the total mass [12,21,7]. Palygorskite is known to be specific to dust particles collected in North Sahara [10,42], while both illite and palygorskite have been identified in dusts form the Middle East [15] and other desert regions of the world [17].

We use the illite from Fithian, Vermillion County, Illinois, U.S.A., which is referenced as American Petroleum Institute (API) reference clay mineral n°35, and named “IF” here. IF was supplied from the Ward's Natural Science collection. The kaolinite from Warren County, Georgia, U.S.A., which is referenced as KGa-2 and named “KG” here, and the palygorskite from Florida, U.S.A. and referenced as P-Fl-1 is named “PF”. KG and PF were supplied by the Clay Minerals Society's Source Clays Repository. The mineral compositions of these reference materials, which are mixed with other mineral impurities, have been described in Seabaugh et al. [45] for the illite, and in Chipera and Bish [8] for the kaolinite and the palygorskite.

Regarding the source desert soils, we chose two soil samples, a Sahelian soil collected in the area of Banizoumbou in Niger (13°31′N, 2°38′E) and hereinafter named “N”; and a Saharan soil collected in Douz in Tunisia (33°25′N, 09°02′E) and hereinafter named “T”. These soil samples were collected from the first centimeters of the top layer of the desert soils, exposed to wind erosion. We work with the < 1 mm sieved soil fractions. These soil samples have already been used as aerosol equivalent samples, previously also sieved [1,32,46] and for generating laboratory aerosols [34].

Dust aerosol samples on filters were generated, following the same laboratory protocol for both the reference mineral powders and the soil samples. We use the GAMEL (“Générateur d’Aérosol Minéral En Laboratoire”) generation system described in Lafon et al. [34]. This device allows for the collection of aerosol particles on filters, from small quantities of desert soils (1 g). Both the size-distributions and the elemental compositions of such produced aerosol samples, compare well with those collected in the ambient atmosphere during local dust events [34]. The size and the elemental compositions of the laboratory generated samples also proved to be repeatable. The experimental conditions, defined by soil quantities, shaking frequency and duration of shaking [34] are displayed in Table 1. Coarse cleaned quartz grains were added in the shaking flask, together with the reference mineral powder, in order to increase shocking and then dispersion of powder aggregates. The dust generation conditions are chosen to enable us to collect several hundred µg of aerosol particles on a Whatman® Nuclepore® filter, equivalent to the amounts of ambient dust aerosols that are typically collected on filters during field campaigns (e.g. [32]). Since filters usually required for XRD measurements are loaded with at least about 1 mg of dust [4], we performed successive sampling experiments to accumulate similar amounts of dust samples on the filters. The mass of aerosol particles collected on the filters was estimated from the total number of particle collected (TSP) measured by an optical particle counter running in parallel with the aerosol sampling and from the total oxide mass measured by X-ray fluorescence (XRF) spectrometry performed on Whatman® Nuclepore® filters collected during a reference generation experiment following Lafon et al. [34]. The estimated mass (M) of the analyzed samples are presented in Table 1, except for KG1 and KG2 for which TSP data were not available. This procedure allows us to perform XRD measurements on low mass samples (from 0.3 to 1.8 mg of aerosol particles). KG1/2/3 samples as well as T1/2/3 will be used to discuss the precision of the XRD measurements.

2.2. Sample preparation for XRD analyses

In order to collect the aerosol particles, each filter sample is deposited in 3 ml of ethanol, in a Teflon® beaker. Two ultrasonic treatments are applied for about 2 min in total. The resulting suspension is transferred in a 50 ml polycarbonate tube and ultra-centrifuging (Beckman Avanti J-26 XP) at 22,500 rpm for 30 min in order to trap most of the particles, including the smallest ones. The supernatant solution is then extracted with a pipette. After the evaporation of the ethanol, 50 µl of deionized water is added to the residue; the resulting suspension is homogenized by sonicating, and deposited on a Si wafer. This step is repeated to recover all the particles from the polycarbonate tube. For XRD measurements, the Si wafer displays a flat and quite linear background diffraction pattern, with no detected diffraction peaks limiting background effects. Such a preparation leads to preferred orientation of the platy minerals, enhancing the diffraction peaks from basal reflections of the clay minerals, also allowing identification of minor amounts of clay phases [3]. The samples prepared by this procedure are hereafter referred to as -waf.

After the first XRD measurement, the powder sample is scraped off the Si wafer using a glass slide, and introduced in a glass capillary (1 mm diameter) to perform the second XRD measurement. The perfectly smooth surface of the Si-wafer allows the full recovery of the matter. The samples prepared following this procedure are hereafter referred to -cap.

Working with aerosolized material avoids coarse aggregates which could affect the random orientation of mineral grains even with the capillary tube rotation. Furthermore, the diameter of the capillary compared to the size of the aerosol particles is large enough to allow the random orientation of the particles. A large number of crystallites is an important requirement for achieving a successful Rietveld refinement [29]. By generating and collecting between 10^6 and 10^8 TSP particles with GAMEL, depending on the samples, we were able to have enough data to perform the Rietveld analysis.

Table 1
GAMEL device experimental setup and estimated mass from each sample generated and collected on Nuclepore® membrane filter from reference mineral powders and desert soils.

Shaken mineral or soil	Soil or mineral quantity (g)	Shaking		Aerosol sample nomenclature	XRD analyzed sample	Estimated aerosol mass (mg)
		Frequency (min^{-1})	Duration (min)			
Illite + quartz	0.5 + 0.5	500	9	IF	IF	1.5
Kaolinite + quartz	0.5 + 0.5	650	9	KG	KG1	–
					KG2	–
					KG3	1.8
Palygorskite + quartz	0.5 + 0.5	500	9	PF	PF	0.3
Niger	1	500	9	N	N	1.4
Tunisia	1	500	9	T	T1	1.4
					T2	0.5
					T3	0.7

2.3. XRD measurements and analyses

X-ray diffraction (XRD) diagrams of the samples are recorded on a Panalytical Empyrean diffractometer equipped with a PIXcel detector (255 active channels) fitted with a Cu anode tube ($K\alpha_1$ = 1.5406 Å) operating at 45 kV and 40 mA. Panalytical Empyrean powder diffractometer is a multi-configuration device with which good measurements can be obtained for a wide variety of polycrystalline samples, as thin layers [6], geological powders [49], or even heterogeneous metallic bulks [35]. Diffractograms are recorded in the 5°–90° 2θ range. Regarding the Si-wafer measurements, the sample holder is a reflection spinner (1 s rotation time). For the capillary mounted samples, a focusing X-ray mirror is used.

Mineral identification is performed using the Highscore Plus 3.0 software and two databases: ICSD (Inorganic Crystal Structure Database) and COD (Crystallography Open Database). We have therefore chosen the Rietveld method to analyze the whole diffraction patterns. The MAUD program (Material Analysis Using Diffraction) is a general X-ray diffraction program based mainly on the Rietveld refinement method [36], applied for quantitative phase analysis in this project. The Rietveld method is a full-pattern analysis that minimizes the difference between experimental and calculated XRD diagrams by a least-squares procedure. Many parameters can be adjusted in the refinement, such as lattice parameters, atomic position, background function, phase fraction, etc. The instrumental influence and absorption effects are taken into account by the analysis of a standard, under the same analytical conditions as for the samples. In this study, we use a Lanthanum hexaboride (LaB6) standard, certified by the National Institute of Standards and Technology (NIST). Using the theoretical crystal structures corresponding to the identified phases, and after loading the experimental data, the software generates a quantitative analysis, with the best Goodness Of Fit (GOF). It is important to know that for a given diffractogram, the GOF can take values between 1 and few tens, and more the GOF approaches unity, the better the fit. It is not possible to compare GOF obtained for two different measurements, so GOF provides a guideline but not a criterium. We subsequently evaluated the quality of the fit by looking at the plot through the simulated points, as well as the plot of the difference between the simulated and the experimental patterns. However, the Rietveld method requires identifying all the crystallized mineral phases. The crystallites must exhibit a random distribution of crystal orientations for the relative intensities of the measured peaks to correspond to the theoretical values.

3. Results and discussion

XRD analysis was performed on the 3 reference minerals (KG, IF, PF) and on 2 laboratory generated dust aerosol particles from desert soils of Tunisia (T) and Niger (N). In order to check the repeatability of the procedure, the KG and T samples were analyzed in triplicate. Also, all samples, collected on Nuclepore® filters, have been analyzed after the two preparation methods previously described (-waf and -cap). The reference materials are essentially composed of single minerals and other minor and trace minerals as impurities. We present and discuss in this section the diffractograms, the mineral phases identified using -waf measurements, the quantification obtained with -cap samples, as well as the differences in peak intensities between -waf and -cap.

3.1. Reference mineral analyses

3.1.1. Kaolinite analyses

The kaolinite (ICSD#98-006-8697) and anatase (ICSD#98-015-6838) mineral phases were identified in the three KG aerosol samples, for both sample preparation methods (-waf, –cap) (Fig. 2). Table 2 provides the peak intensities and their differences from the theoretical values for the 3 samples KG1/2/3. Disorders in the crystal structure as well as the presence of many well-crystallized phases are responsible for the various diffraction profiles for kaolinite minerals described in literature [13]. As a consequence, many theoretical ICSD files exist for the kaolinite, with varying theoretical peak intensities. The theoretical intensities applied as references in Table 2 are mean values from 11 ICSD files.

Kaolinite diffraction peaks and their relative intensities for KG1/2/3-waf, show strong preferred orientation, since the three measurements display, for the (010) peak (19.8° 2θ), a relative deviation from the theoretical intensity of 95–97% was found. Measurements in the capillaries were conducted on the three same KG samples (KG1/2/3-cap). The deviation from theoretical values appears to be much less for capillary measurements than for the wafer measurements. We also note that measurements made on three similar samples show similar intensities. Indeed the standard deviations of the mean intensities from the three repetitions for the (010) (19.8° 2θ) and (002) (24.9° 2θ) peaks are respectively 0.5% and 5.2% for capillary repetitions and 3.1% and 5.1% for wafer measurements. The excellent repeatability is a distinct advantage of the capillary measurements.

We obtain high quality MAUD fit for KG. In fact, the observed and calculated patterns are similar, as illustrated in Fig. 2, and the low GOF value of 3. Quantitative analyses were conducted on the three obtained diffractograms. The results show averages of 95.5% (relative standard deviation (RSD) 1%) of kaolinite and an average of 4.5% (RSD 15%) of anatase impurity for the three measurements.

The KGa-2 is known to be composed of kaolinite and a small amount of anatase [8], with respectively 96% of kaolinite and 3% of anatase, as well as about 1% of crandalite and/or illite. The measured compositions of the KG aerosol samples are similar to those obtained on bulk powders by various authors (e.g. [8,2]). We can safely assume that the procedure we adopted is repeatable, and reliable for quantification of kaolinite in small aerosol samples.

3.1.2. Illite analyses

Four phases are identified in the IF-waf sample, illite (ICSD#98-009-0144), quartz (ICSD#98-009-0145), jarosite (ICSD#98-016-0404) and kaolinite (ICSD#98-006-8697). Only 3 phases are detected by the IF-cap method, i.e. illite, quartz and jarosite. Due to both the small kaolinite proportion, and a weak signal from the random orientation of crystallites, it can be expected that this mineral was not detected by the capillary measurement. Illite, similar to kaolinite, has a strong preferential orientation when deposited on Si-wafer. The theoretical intensities used for the illite comparison are from the ICSD file (ICSD#98-009-0144). The relative intensities obtained with the capillary measurement are also much closer to the theoretical intensities than those obtained from Si-waferdeposit measurements (Table 2). Indeed, the important deviation from theoretical intensities of the (002) and (004) peaks (at 8.8° 2θ and 17.7° 2θ) for the wafer measurements (respectively 880% and 172%) show the strong preferential orientation while the relatively low values of this deviation of the same peaks for capillary measurements (respectively 21% and 49%) reflect the good quality of the signal obtained with this sample presentation. Our approach, with -waf and -cap measurements, points to the advantage of the capillary mounted measurements for the assessment of platy minerals such as illite.

Moreover, for the IF-cap sample, the good agreement between the experimental pattern and the MAUD Rietveld refinement (Fig. SI-1, with a GOF value of 4) justifies using measurements on capillaries for quantitative mineral analysis. The analysis of IF-cap shows 84.3% illite, 10.5% quartz and 5.2% jarosite. Molloy and Kerr [37], Hogg et al. [23] and [45] also identified 3 minor phases in illite Fithian powder. Quartz and kaolinite were always detected at trace levels, but a fourth phase was identified as montmorillonite [37], feldspar [23], or jarosite (Sebaugh et al., 2006). Our results showing about 6% of jarosite (which is the only specie they quantified by XRD) are in good agreement with those of Sebaugh et al. (2006). As above, the aerosol of reference

Table 2
Peak positions, theoretical intensities, intensities obtained from the Si-wafer and capillary tube preparation methods, and the relative deviations from the theoretical intensities (in %) for kaolinite KG, illite IF and palygorskite PF.

	Peak Position (deg.) / d-spacing (Å)	Miller indices	Theoretical Intensity	Wafer Intensity	Relative Deviation from the Theoretical Intensity (%)	Capillary Intensity	Relative Deviation from the Theoretical Intensity (%)
KG1*	12.4 / 7.1	(001)	100.0	100.0	–	100.0	–
	19.8 / 4.5	(010)	53.7 (10.3)	1.5	97.2	39.4	26.6
	24.8 / 3.6	(002)	65.5 (9.9)	55.1	15.9	75.3	15.0
KG2*	12.4 / 7.1	(001)	100.0	100.0	–	100.0	–
	19.8 / 4.5	(010)	53.7 (10.3)	2.5	95.3	39.3	26.8
	24.8 / 3.6	(002)	65.5 (9.9)	49.4	24.6	83.6	27.6
KG3*	12.4 / 7.1	(001)	100.0	100.0	–	100.0	–
	19.8 / 4.5	(010)	53.7 (10.3)	1.9	96.5	44.7	16.8
	24.8 / 3.6	(002)	65.5 (9.9)	59.8	8.7	84.7	29.3
IF**	8.8 / 10,0	(002)	56.1	549.5	880.0	44.3	21.1
	17.7 / 5.0	(004)	34.9	95.0	172.0	17.8	49.2
	19.8 / 4.5	(11-1)	100.0	100.0	–	100.0	–
PF***	8.5 / 10.4	(101)	100.0	100.0	–	100.0	–
	13.9 / 6.4	(002)	15.5	7.9	49.0	8.1	47.7
	16.4 / 5.4	(301)	22.1	4.9	77.8	7.1	67.9
	19.8 / 4.5	(400)	23.8	7.5	68.5	21.7	8.8
	20.8 / 4.3	(211)	25.0	5.5	78.0	17.0	32.0

*Theoretical intensities are mean values from 11 ICSD files. The standard deviation is denoted in brackets. **Theoretical intensity corresponding to the ICSD#98-009-0144 file. ***Theoretical intensities corresponding to the ICSD#98-009-7695 file.

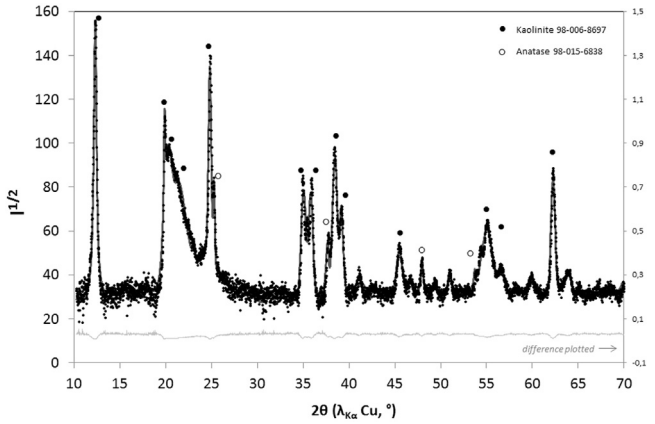

Fig. 2. Diffractogram obtained by capillary measurement of the aerosol sample generated from the kaolinite reference mineral (KG-cap). The square root of the detected intensity for the y-axis allows a better visibility of the low intensity peaks. The black dots correspond to the experimental data and the red curve to the simulated data by MAUD software (GOF = 3.0). The grey curve is the difference between experimental and simulated data. The peaks corresponding to the kaolinite are indicated by solid black circles, those of the anatase by white circles. (For interpretation of the references to color in this figure legend, the reader is referred to the web version of this article.).

mineral is similar to the analyzed bulk powders. We can safely assume the reliability of illite concentrations as measured on capillary mounted samples.

3.1.3. Palygorskite analyses

Four mineral phases were detected from the Si-wafer powder mounts, i.e. palygorskite (ICSD#98-009-7695), smectite (ICSD#98-016-1171), quartz (ICSD#98-009-0145) and anorthite (ICSD#98-003-4942). Smectite was not detected from the capillary measurements (Fig. SI-2 and insert). Smectite is always difficult to detect by XRD [3] since this mineral is often poorly crystallized. If detected, the signal is weakly resolved, showing broad peaks and low signal-to-noise ratios (see insert in Fig. SI-2). The combined effect of the poor crystallization and the low concentration of the smectite leads to a weak signal using a capillary sample mount. For these reasons, the capillary mount did not allow for the quantification of smectite in dust aerosol samples.

Regarding the peak intensity of the palygorskite itself, the measurement made from the capillary mount displays a better agreement with the ICSD#98-009-7695 file than the one made with the Si-wafer, especially for the (400) peak at 19.8° 2θ. Its relative deviation from theoretical intensity is 8.8% for the capillary sample mount while it is 68.5% for Si-wafer sample mount. The MAUD Rietveld fit performed on PF-cap models a composition of 85.8% palygorskite 5.4% quartz and 8.8% anorthite (calcic feldspar), with a GOF of 2.7. Chipera and Bish [8] analyzed 79% palygorskite, 11% smectite, 6.0% quartz and 5% feldspar for the same reference material (PFl-1). Besides the limitation for the smectite detection at low concentrations, our results are in fairly good agreement with the results of Chipera and Bish [8]. Thus, the procedure is suitable for quantification of palygorskite in small aerosol samples.

3.2. Mineralogical characterization of laboratory generated dust aerosol particles

The procedure described above provided the relative X-ray peak intensities for kaolinite, illite and palygorskite compared to theoretical values, and confidence in our quantitative XRD results. The subsequent step was to analyze more complex aerosol samples, generated from desert soils. Such samples are considered to represent a mineral mixture that can be found in atmospheric aerosols. Six mineral phases were identified in the Tunisian Si-wafer samples, i.e. calcite, dolomite, quartz, illite, palygorskite and kaolinite, and four phases in the Niger sample, i.e. quartz, kaolinite, microcline (potassium feldspar) and illite. All phases were also identified in the capillary mounts.

Fig. 3 shows the fit obtained for the T-cap sample with a GOF of 1.8 (the diffractogram for N-cap is presented in Fig. SI-3 with a GOF of 1.2). Curves are fitted from the best ICSD files, as shown in the legend.

Measurements are performed on 3 Tunisian samples to assess the repeatability of the measurements. Quantitative results of the Rietveld refinement performed on the three Tunisian samples, expressed as mass proportions, and their mean concentration are presented in Table 3. The associated uncertainties are calculated by the MAUD software for each sample. The standard deviation about the mean concentration of the three capillary measurements, T Mean ± SD (%) (Table 3), is a measure of the repeatability of the sample preparation and the measurement. We observe that for the calcite which is the major phase (62.4%), the standard deviation is small (2.7%). For the minor phases such as quartz, kaolinite, illite and dolomite, the standard deviation lies between 0.3% and 1.1%. The higher SD for the palygorskite (1.8%,

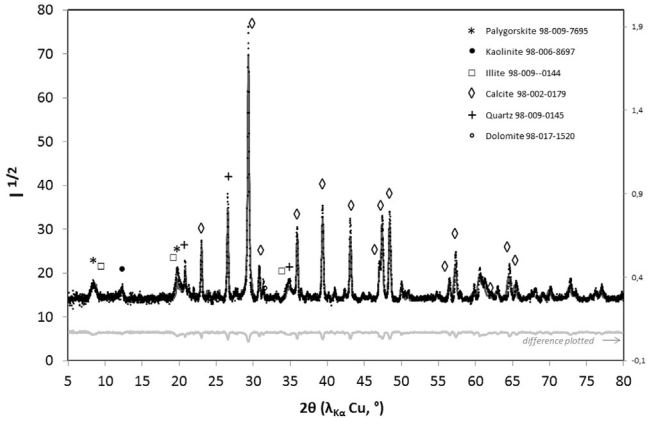

Fig. 3. Diffractogram obtained by capillary measurement of the aerosol sample generated from the Tunisian soil (T-cap). The square root of the detected intensity for the y-axis allows a better visibility of the low intensity peaks. The black dots correspond to the experimental data and the red curve to the simulated data by MAUD software (GOF = 1.8). (For interpretation of the references to color in this figure legend, the reader is referred to the web version of this article.).

corresponding to RSD of 31%) can be explained by the partial overlap of the illite and palygorskite diffraction peaks, especially difficult to resolve at low mineral concentrations. Some authors reported qualitative results of aerosols and soils from desert source regions [17]. The less than 20 μm diameter fraction obtained by dry sieving of the soil of Douz (same soil as the one we used to generate T) has been analyzed by Guieu et al. [22]. The authors reported the dominance of quartz (40%) and calcite (30%) and traces of dolomite. The total clay fraction was estimated to 25% and contained mainly illite and kaolinite with traces of palygorskite. This coarse fraction (up to 20 μm) of the soil is expected to be enriched in quartz particles compared to a typical aerosol particle size sample, which is consistent with our results.

The composition of the Niger aerosol presents less mineralogical phases than the Tunisian one, with 4 detected phases reported in Table 3: quartz (48.6 ± 3.1%), kaolinite (26.4 ± 0.5%), microcline (feldspar) (12.5 ± 0.7%) and illite (12.5 ± 0.5%). Lafon [31] found that a wind tunnel aerosol generated from the same Banizoumbou soil as the one used in this study for N contained mainly quartz (+ + +), illite (+ +), kaolinite (+ + + + +), feldspar (+) and no calcite. The number of + symbol reflects the relative peak intensities but cannot be used as quantitative information since the analysis was performed on sample mounts with preferred mineral orientations. Even if the measurements of Lafon [31] are expected to overestimate the abundance of kaolinite, particularly inclined to orientation, our results point out the same mineral phases.

Table 4
Estimated mass of quantified minerals by XRD for each sample in μg (N: Niger dust, T1/T2/T3: Tunisian dust).

Sample mineral masses (μg)	N	T1	T2	T3
Kaolinite	370	94	25	43
Illite	175	188	57	85
Palygorskite	–	108	28	29
Quartz	680	118	46	64
Calcite	–	829	320	447
Dolomite	–	64	25	32
Microcline	175	–	–	–

From the total mass for each sample (Table 1) and each mineral phase quantified by XRD analysis, the corresponding mass of each mineral in samples was calculated. These values are presented in the Table 4. This calculation shows that we were able to assess quantitative mass concentrations of minerals in aerosol samples collected on Nuclepore® filters, as low as 46 μg, 25 μg, 175 μg and 25 μg, respectively for quartz, calcium carbonates, feldspars and clays.

4. Conclusion

An analytical method and X-Ray Diffraction (XRD) measurements are presented to quantify the mineralogical composition of low mass aerosol particle samples. Three references minerals, kaolinite, illite and palygorskite which are commonly present in desert dust aerosols as well as laboratory generated dust aerosols from desert soils were studied. XRD measurements of these samples mounted in rotating glass capillaries were quantified by the Rietveld refinement method. By working on both oriented and randomly oriented samples, we were able to identify and quantify mineral species. The Rietveld refinement is independent of the instrument and does not require the use of internal standards. Its use for low mass samples provides a novel method for the analysis of the mineralogical composition of aerosols collected on Nuclepore® filters. The measurements obtained by this procedure are repeatable, and the identification of the mineral phases of the reference materials is in agreement with theoretical values from literature. The quantification of smectite by XRD remains difficult. Nevertheless, its presence can be detected from the first step measurement made on a Si-wafer, in which case the smectite diffraction peak is clearly identifiable. This method allows us to quantify most of the crystalline phases of low mass dust mineral samples, including clay minerals, even in low concentrations (between 5% and 10% in T-cap sample), with an unprecedented accuracy. This procedure can also be applied to ambient aerosols collected in the field in order to assess their mineralogical compositions.

Table 3
Quantitative analyze of T-cap and N-cap diffractograms for the Tunisian and Niger dust samples. The Maud software gives an uncertainty on the result of each mineral phase, indicated in this table for the 3 repeats. The uncertainty resulting from the repetition (including both the sample and method variability) is indicated (SD).

	Tunisia				Niger
Mineral	T1-cap (%)	T2-cap (%)	T3-cap (%)	T Mean ± SD (%)	N-cap (%)
Calcite	59.2 ± 3.1	64.0 ± 3.4	63.9 ± 3.1	62.4 ± 2.7	–
Palygorskite	7.7 ± 0.7	5.5 ± 0.4	4.1 ± 0.3	5.8 ± 1.8	–
Quartz	8.4 ± 0.5	9.2 ± 0.2	9.2 ± 0.2	8.9 ± 0.5	48.6 ± 3.1
Kaolinite	6.7 ± 0.5	5.0 ± 0.4	6.1 ± 0.3	5.9 ± 0.5	26.4 ± 0.5
Illite	13.4 ± 0.6	11.3 ± 0.7	12.2 ± 0.7	12.3 ± 1.1	12.5 ± 0.5
Dolomite	4.6 ± 0.3	5.0 ± 0.2	4.5 ± 0.2	4.7 ± 0.3	–
Microcline	–	–	–	–	12.5 ± 0.7

Acknowledgments

The FERATMO and FERATMO + projects were supported by the French national scientific program LEFE/CHAT of the INSU CNRS. We also would like to thank an anonymous referee for its helpful comments.

Appendix A. Supporting information

Supplementary data associated with this article can be found in the online version at http://dx.doi.org/10.1016/j.talanta.2018.03.059.

References

[1] C. Aghnatios, R. Losno, F. Dulac, A fine fraction of soil used as an aerosol analogue during the DUNE experiment: sequential solubility in water with, decreasing pH step-by-step, Biogeosciences 11 (2014) 4627–4633.
[2] C. Belviso, F. Cavalcante, A. Lettino, S. Fiore, A and X-type zeolites synthesized from kaolinite at low temperature, Appl. Clay Sci. 80–81 (1993) 162–168.
[3] G.W. Brindley, G. Brown, Crystal structures of clay minerals and their X-ray identification, Miner. Soc. Monogr. Lond. 5 (1980) 495.
[4] S. Caquineau, M.C. Magonthier, A. Gaudichet, L. Gomes, An improved procedure for the X-ray diffraction analysis of low-mass atmospheric dust samples, Eur. J. Mineral. (1997) 157–166.
[5] S. Caquineau, A. Gaudichet, L. Gomes, M. Legrand, Mineralogy of Saharan dust transported over northwestern tropical Atlantic Ocean in relation to source regions, J. Geophys. Res. 107 (D15) (2002) 4251.
[6] S. Chaguetmi, N. Sobti, P. Decorse, L. Mouton, S. Nowak, F. Mammeri, S. Achour, S. Ammar, Visible-light photocatalytic performances of TiO2 nanobelts decorated with iron oxide nanocrystals, RSC Adv. 6 (2016) 114843–114851.
[7] R. Chester, L.R. Johnson, Atmospheric dusts collected off the West African Coast, Nature 229 (1971) 105–107.
[8] S.J. Chipera, D.L. Bish, Baseline studies of the clay minerals society source clays: powder X-ray diffraction analyses, Clays Clay Miner. 49 (5) (2001) 398–409.
[9] F.H. Chung, Quantitative interpretation of X-ray diffraction patterns of mixtures. III. Simultaneous determination of a set of reference intensities, J. Appl. Crystallogr. 8 (1) (1975) 17–19.
[10] G. Coude-Gaussen, P. Rognon, G. Bergametti, L. Gomes, B. Strauss, J.M. Gros, M.N. Le Coustumer, Saharan dust on Fuerteventura Island (Canaries): chemical and mineralogical characterisitcs, air mass trajectories, and probable sources, J. Geophys. Res. 92 (D8) (1987) 9753–9771.
[11] D.M. Cwiertny, J. Baltrusaitis, G.J. Hunter, A. Laskin, M.M. Scherer, V.H. Grassian, Characterization and acid-mobilization study of iron-containing mineral dust source materials, J. Geophys. Res. 113 (D5) (2008).
[12] A.C. Delany, A.C. Delany, D.W. Parkin, J.J. Griffin, E.D. Goldberg, B.E.F. Reimann, Airborne dust collected at Barbados, Geochim. Cosmochim. Acta 31 (5) (1967).
[13] S. DeLuca, M. Slaughter, Existence of multiple kaolinite phases and their relationship to disorder in kaolin minerals, Am. Mineral. 70 (1985) 149–158.
[14] N.J. Elton, P.D. Salt, Particle statistics in quantitative X-Ray diffractometry, Powder Diffr. 11 (3) (1996) 218–229.
[15] J.P. Engelbrecht, E.V. McDonald, J.A. Gillies, R.K.M. Jayanty, G. Casuccio, A.W. Gertler, Characterizing mineral dusts and other aerosols from the Middle East – Part 1: ambient sampling, Inhal. Toxicol. 21 (4) (2009) 297–326, http://dx.doi.org/10.1080/08958370802464273.
[16] J.P. Engelbrecht, J.A. Gillies, V. Etyemezian, H. Kuhns, S.E. Baker, D. Zhu, G. Nikolich, S.D. Kohl, Controls on mineral dust emissions at four arid locations in the western USA, Aeolian Research 6 (2012) 41–54.
[17] J.P. Engelbrecht, H. Moosmüller, S. Pincock, R.K.M. Jayanty, T. Lersch, G. Casuccio, Technical note: mineralogical, chemical, morphological, and optical interrelationships of mineral dust re-suspensions, Atmos. Chem. Phys. 16 (2016) 10809–10830, http://dx.doi.org/10.5194/acp-16-10809-2016.
[18] J.P. Engelbrecht, G. Stenchikov, P.J. Prakash, T. Lersch, A. Anisimov, I. Shevchenko, Physical and chemical properties of deposited airborne particulates over the Arabian Red Sea coastal plain, Atmos. Chem. Phys. 17 (2017) 11467–11490, http://dx.doi.org/10.5194/acp-17-11467-2017.
[19] P. Formenti, J.L. Rajot, K. Desboeufs, S. Caqineau, S. Chevaillier, S. Nava, A. Gaudichet, E. Journet, S. Triquet, S. Alfaro, M. Chiari, J. Haywood, H. Coe, E. Highwood, Regional variability of the composition of mineral dust from western Africa: results from the AMMA SOP0/DABEX and DODO field campaigns, J. Geophys. Res. 113 (2008) D00C13.
[20] P. Formenti, S. Caquineau, S. Chevaillier, A. Klaver, K. Desboeufs, J.-L. Rajot, S. Belin, V. Briois, Dominance of goethite over hematite in iron oxides of mineral dust from Western Africa: quantitative partitioning by X-ray absorption spectroscopy, J. Geophys. Res. 119 (2014) (12740-1275).
[21] R.A. Glaccum, J.M. Prospero, Saharan aerosols over the tropical north Atlantic mineralogy, Mar. Geol. 37 (3) (1980) 295–321.
[22] C. Guieu, F. Dulac, K. Desboeufs, T. Wagener, et al., Large clean mesocosms and simulated dust deposition: a new methodology to investigate responses of marine oligotrophic ecosystems to atmospheric inputs, Biogeosciences 7 (2010) 2765–2784.
[23] A.J.C. Hogg, N.J. Pearson, A.E. Fallick, Pretreatment of Fithian illite for oxygen isotop analysis, Clay Miner. 28 (1993) 149–152.
[24] IPCC, S. Solomon, et al. (Ed.), Climate Change 2007: The Physical Science Basis, Contribution of Working Group I to the Fourth Assessment Report of the Intergovernmental Panel on Climate Change, Cambridge Univ. Press, Cambridge, U. K, 2007.
[25] E. Journet, K.V. Desboeufs, S. Caquineau, J.-L. Colin, Mineralogy as a critical factor of dust iron solubility, Geophys. Res. Lett. 35 (2008) L07805.
[26] K. Kandler, N. Benker, U. Bundke, E. Cuevas, M. Ebert, et al., Chemical composition and complex refractive index of Saharan Mineral Dust at Iza˜na, Tenerife (Spain) derived by electron microscopy, Atmos. Environ. 41 (2007) 8058–8074.
[27] K. Kandler, L. Schütz, C. Deutscher, et al., Size distribution, mass concentration, chemical and mineralogical composition and derived optical parameters of the boundary layer aerosol at Tinfou,Morocco, during SAMUM2006, Tellus 61B (2009) 32–50.
[28] A. Klaver, P. Formenti, S. Caquineau, S. Chevaillier, P. Ausset, G. Calzolai, S. Osborne, B. Johnson, M. Harrison, O. Dubovik, Physico-chemical and optical properties of Sahelian and Saharan mineral dust: in situ measurements during the GERBILS campaign, Q. J. R. Meteorol. Soc. (2011), http://dx.doi.org/10.1002/qj.889.
[29] H.P. Klug, L.E. Alexander, X-Ray Diffraction Procedures, 2nd edition, John Wiley & Sons, New York, 1974.
[30] B.J. Krueger, V.H. Grassian, J.P. Cowin, A. Laskin, Heterogeneous chemistry of individual mineral dust particles from different dust source regions: the importance of particle mineralogy, Atmos. Environ. 38 (2004) 6253–6261.
[31] S. Lafon, Les Oxydes de fer Dans L'aerosol Desertique en Relation Avec Ses Proprietes Optiques: Caracterisation Physico-Chimique de Poussieres Minerales Generees en Soufflerie (Ph.D. thesis), Univ. Paris 12, Val-de-Marne, Creteil, France, 2004, p. 325.
[32] S. Lafon, J. Rajot, S. Alfaro, A. Gaudichet, Quantification of iron oxides in desert aerosol, Atmos. Environ. 38 (2004) 1211–1218.
[33] S. Lafon, I.N. Sokolik, J.L. Rajot, S. Caquineau, A. Gaudichet, Characterization of iron oxides in mineral dust aerosols: implications for light absorption, J. Geophys. Res. 111 (2006) D21207.
[34] S. Lafon, S. Alfaro, S. Chevaillier, J.-L. Rajot, A new generator for mineral dust aerosol production from soil samples in the laboratory: GAMEL, Aeolian Res. 15 (2014) 319–334.
[35] E. Lebrun, P. Svec, S. Nowak, B. Denand, Y. Millet, F. Prima, Phase transformations of TIMETAL-18 as a new titanium alloy with bimodal microstructure, Adv. Mater. Res. 922 (2014) 418–423.
[36] L. Lutterotti, S. Matthies, H.-R. Wenk, MAUD: a friendly Java program for material analysis using diffraction, IUCr: Newsl. CPD 21 (1999) 14–15.
[37] M.W. Molloy, P.F. Kerr, Diffractometer patterns of A.P.I. reference clay minerals, Am. Mineral. 46 (1961) 583–605.
[38] H. Moosmüller, J.P. Engelbrecht, M. Skiba, G. Frey, R.K. Chakrabarty, W.P. Arnott, Single scattering albedo of fine mineral dust aerosols controlled by iron concentration, J. Geophys. Res. 117 (2012) D11210, http://dx.doi.org/10.1029/2011JD016909.
[39] D.M. Moore, R.C.J. Reynolds, X-Ray Diffraction and the Identification and Analysis of Clay Minerals, Oxford University Press, Oxford, New York, 1997.
[40] J.M. Prospero, P. Ginoux, O. Torres, S.E. Nicholson, T.E. Gill, Environmental characterization of global sources of atmospheric soil dust identification with the Nimbus 7 Total Ozone Mapping Spectrometer (TOMS) absorbing aerosol product, Rev. Geophys. 40 (2002) 1002, http://dx.doi.org/10.1029/2000RG000095.
[41] H.M. Rietveld, Line profiles of neutron powder diffraction peaks for structure refinement, Acta Cryst. 22 (1967) p151–p152.
[42] D. Scheuvens, L. Schütz, K. Kandler, M. Ebert, S. Weinbruch, Bulk composition of northern African dust and its source sediments—a compilation, Earth-Sci. Rev. 116 (2013) 170–194.
[43] A.W. Schroth, J. Crusius, E.R. Sholkovitz, B.C. Bostick, Iron solubility driven by speciation in dust sources to the ocean, Nat. Geosci. 2 (5) (2009) 337–340.
[44] M. Schulz, J.M. Prospero, Baker, et al., Atmospheric transport and deposition of mineral dust to the ocean: implications for research needs, Environ. Sci. Technol. 46 (19) (2012) 10390–10404.
[45] J.L. Seabaugh, H. Dong, R.K. Kukkadapu, D.D. Eberl, J.P. Morton, J. Kim, Microbial reduction of fe(III) in the Fithian and Muloorina illites: contrasting extents and rates of bioreduction, Clays Clay Miner. 54 (N°1) (2006) 67–79.
[46] Z. Shi, M.D. Krom, S. Bonneville, A.R. Baker, T.D. Jickells, L.G. Benning, Formation of iron nanoparticles and increase in iron reactivity in the mineral dust during simulated cloud processing, Environ. Sci. Technol. 43 (2009) 6592–6596.
[47] I.N. Sokolik, O.B. Toon, Incorporation of the mineralogical composition into models of the radiative properties of mineral aerosol from UV to IR wavelengths, J. Geophys. Res. 104 (D8) (1999) 9423–9444.
[48] R.A. Young, The Rietveld Method, IUCr Monographs on Crystallography, Oxford University Press, New York, 1993.
[49] I. Zelano, Y. Sivry, C. Quantin, A. Gelabert, M. Tharaud, S. Nowak, J. Garnier, Study of Ni exchangeable pool speciation in ultramafic and minig environments with isotopic exchange kinetic data and models, Appl. Geochem. 64 (2016) 146–156.
[50] F. Zimmermann, S. Weinbruch, L. Schütz, H. Hofmann, M. Ebert, K. Kandler, A. Worringen, Ice nucleation properties of the most abundant mineral dust phases, J. Geophys. Res. 113 (D23) (2008).